Molecular Biology of the Cell
Vol. 17, 4027–4038, September 2006

BLOC-1 Interacts with BLOC-2 and the AP-3 Complex to Facilitate Protein Trafficking on Endosomes[D]

Santiago M. Di Pietro,* Juan M. Falcón-Pérez,* Danièle Tenza,† Subba R.G. Setty,‡ Michael S. Marks,‡ Graça Raposo,† and Esteban C. Dell'Angelica*

*Department of Human Genetics, University of California, Los Angeles, CA 90095; †Institut Curie, Centre National de la Recherche Scientifique-Unité Mixte de Recherche 144, Paris 75248, France; and ‡Department of Pathology and Laboratory Medicine, University of Pennsylvania, Philadelphia, PA 19104

Submitted May 3, 2006; Revised June 26, 2006; Accepted July 5, 2006
Monitoring Editor: Sandra Schmid

The adaptor protein (AP)-3 complex is a component of the cellular machinery that controls protein sorting from endosomes to lysosomes and specialized related organelles such as melanosomes. Mutations in an AP-3 subunit underlie a form of Hermansky-Pudlak syndrome (HPS), a disorder characterized by abnormalities in lysosome-related organelles. HPS in humans can also be caused by mutations in genes encoding subunits of three complexes of unclear function, named biogenesis of lysosome-related organelles complex (BLOC)-1, -2, and -3. Here, we report that BLOC-1 interacts physically and functionally with AP-3 to facilitate the trafficking of a known AP-3 cargo, CD63, and of tyrosinase-related protein 1 (Tyrp1), a melanosomal membrane protein previously thought to traffic only independently of AP-3. BLOC-1 also interacts with BLOC-2 to facilitate Tyrp1 trafficking by a mechanism apparently independent of AP-3 function. Both BLOC-1 and -2 localize mainly to early endosome-associated tubules as determined by immunoelectron microscopy. These findings support the idea that BLOC-1 and -2 represent hitherto unknown components of the endosomal protein trafficking machinery.

INTRODUCTION

Early endosomes and their associated tubules constitute a major sorting station within the cell, from which proteins can be targeted to several possible destinations including the plasma membrane, the *trans*-Golgi network, and both limiting and intralumenal membranes of late endosomes and lysosomes (for recent reviews see Gruenberg and Stenmark, 2004; Perret *et al.*, 2005). Given the multiplicity of these sorting events, it is not surprising that endosomal protein trafficking is controlled by a highly complex molecular machinery, of which many components are still being uncovered (Perret *et al.*, 2005). In certain cell types, some components of the ubiquitous endosomal sorting machinery are "diverted" to serve in the targeting of proteins to specialized lysosome-related organelles that coexist with lysosomes, such as the melanosomes of melanocytes and retinal pigment epithelial cells (reviewed by Raposo *et al.*, 2002). Even when the machinery for trafficking to lysosome-related organelles represents a subset of the ubiquitous machinery, accumulating evidence indicates that it is in itself complex (Raposo *et al.*, 2002; Theos *et al.*, 2005).

A relevant example is that of the heterotetrameric adaptor protein (AP)-3 complex. In fibroblasts, AP-3 serves in a route for trafficking of lysosome-associated membrane proteins (LAMPs) from early endosome-associated tubules to late endosomes and lysosomes (Peden *et al.*, 2004 and references therein), whereas in melanocytes it mediates the trafficking of the key melanogenic enzyme, tyrosinase, to maturing melanosomes (Huizing *et al.*, 2001; Theos *et al.*, 2005). Consistent with a role for AP-3 in the sorting of proteins to melanosomes and other lysosome-related organelles (e.g., platelet dense granules, azurophil, and lytic granules), mutations in the human gene encoding the β3A subunit of the complex underlie Hermansky-Pudlak syndrome (HPS) type 2, a recessive disorder characterized by albinism, prolonged bleeding, and innate immune defects (Dell'Angelica *et al.*, 1999b; Clark *et al.*, 2003; Fontana *et al.*, 2006). Some components of the ubiquitous "AP-3–dependent pathway" have been identified, including ARF1 and its GTPase-activating protein, AGAP1, clathrin, and phosphatidylinositol-4-kinase type II α (Dell'Angelica *et al.*, 1998; Faúndez *et al.*, 1998; Ooi *et al.*, 1998; Nie *et al.*, 2003; Salazar *et al.*, 2005b). However, published evidence suggests that AP-3 may also function independently of clathrin (Faúndez *et al.*, 1998; Peden *et al.*, 2002), and the significance of ARF1, AGAP1, and phosphatidylinositol-4-kinase type II α for AP-3–dependent trafficking to melanosomes and other lysosome-related organelles remains to be ascertained. Moreover, an alternative route for AP-3–independent trafficking of tyrosinase from endosomes to melanosomes has been described (Theos *et al.*, 2005) and

This article was published online ahead of print in *MBC in Press* (http://www.molbiolcell.org/cgi/doi/10.1091/mbc.E06–05–0379) on July 12, 2006.

[D] The online version of this article contains supplemental material at *MBC Online* (http://www.molbiolcell.org).

Address correspondence to: Esteban C. Dell'Angelica (Edellangelica@mednet.ucla.edu).

Abbreviations used: AP, adaptor protein; BLOC, biogenesis of lysosome-related organelles complex; EEA1, early endosome antigen 1; HPS, Hermansky-Pudlak syndrome; HRP, horseradish peroxidase; LAMP, lysosome-associated membrane protein; mAb, monoclonal antibody; siRNA, small interference RNA; Tf, transferrin; TfR, transferrin receptor; Tyrp1, tyrosinase-related protein 1.

the trafficking of tyrosinase-related protein 1 (Tyrp1) to melanosomes has been proposed to be entirely independent of AP-3 function (Huizing *et al.*, 2001). Consequently, additional components of AP-3–dependent and –independent trafficking pathways to melanosomes are likely to exist.

Obvious candidate components of the machinery that mediates sorting to melanosomes are the products of genes associated with other forms of HPS. At least seven types of HPS besides type 2 have been described in humans, each of them caused by recessive mutations in the gene encoding a subunit of any of three stable protein complexes, named biogenesis of lysosome-related organelles complex (BLOC)-1, -2, and -3 (for a recent review, see Wei, 2006). Thus, the genes defective in HPS types 7 and 8 (the dysbindin and BLOS3 proteins, respectively) encode two of the eight known subunits of BLOC-1, the products of the genes mutated in HPS types 3, 5, and 6 are components of BLOC-2, and the products of the genes defective in HPS types 1 and 4 are subunits of BLOC-3 (Table 1). Intriguingly, the *DTNBP1* gene defective in HPS type 7 and encoding the dysbindin subunit of BLOC-1 is also considered a promising candidate susceptibility gene for schizophrenia, a severe psychiatric disease with significant, but complex, genetic involvement (reviewed by Harrison and Weinberger, 2005; Norton *et al.*, 2006). Like AP-3, all of the BLOCs are expressed in a wide variety of cell types (including fibroblasts and melanocytes) and exist in both soluble and peripheral membrane protein forms (reviewed by Dell'Angelica, 2004; Li *et al.*, 2004; Wei, 2006).

The aim of this work was to determine the functional relationships between the different BLOCs and AP-3 by means of biochemical, genetic, and cell biological approaches. Although published evidence indicates that AP-3 and BLOC-3 act independently of each other (Dell'Angelica *et al.*, 2000; Feng *et al.*, 2002; Martina *et al.*, 2003), the functional relationships between any of them and BLOC-1 and -2 have remained largely unexplored. In this article, we report the existence of physical and functional interactions between BLOC-1, BLOC-2, and AP-3, with a role in protein trafficking on endosomes.

Table 1. Known subunits of AP-3 and the BLOCs and relevant reagents used in this study

		Reagents	
Complex	Subunit	Mutant mouse	Antibodies[a]
AP-3	β3A[b]	Pearl (*pe*)	β3A1
	δ	—	mAb S4A, mAb clone 18[c]
	μ3A[b]	—	mAb anti-p47A
	σ3(A/B)	—	Anti-σ3
BLOC-1	Pallidin	Pallid (*pa*)	Anti-PA, mAb anti-pallidin
	Dysbindin	—	Anti-dysbindin
	BLOS3	—	Anti-BLOS3
	BLOS2	—	—
	BLOS1	—	—
	Cappuccino	—	—
	Muted	—	—
	Snapin	—	—
BLOC-2	HPS3	Cocoa (*coa*)	HP3c
	HPS5	—	—
	HPS6	—	HP6d, anti-Ru[d]
BLOC-3	HPS1	Pale ear (*ep*)	—
	HPS4	—	HP4c, mAb anti-HPS4

[a] Affinity-purified rabbit polyclonal antibodies except for those denoted as mouse mAbs and anti-Ru (crude rabbit antiserum).

[b] Component of ubiquitous form of AP-3.

[c] S4A was used for immunoelectron microscopy and clone 18 for immunoblotting.

[d] HP6d and anti-Ru were used to probe for human and mouse HPS6, respectively.

MATERIALS AND METHODS

Antibodies

Rabbit polyclonal antibodies to the following proteins have been described: AP-3 subunits σ3 and β3A (Dell'Angelica *et al.*, 1997a, 1997b), AP-4 subunit ε (Dell'Angelica *et al.*, 1999a), BLOC-1 subunits pallidin, dysbindin, and BLOS3 (Falcón-Pérez *et al.*, 2002; Starcevic and Dell'Angelica, 2004), BLOC-2 subunits HPS3 and HPS6 and BLOC-3 subunit HPS4 (Nazarian *et al.*, 2003; Di Pietro *et al.*, 2004). Rabbit antisera to the Ru/HPS6 subunit of mouse BLOC-2 (Gautam *et al.*, 2004) and early endosomal antigen 1 (EEA1; Mills *et al.*, 1998) were gifts from Richard T. Swank and Michael J. Clague, respectively. The monoclonal antibody (mAb) against pallidin was described (Nazarian *et al.*, 2006). The mAb S4A against the δ subunit of AP-3 (Peden *et al.*, 2004) was a gift from Andrew A. Peden. The mouse mAb to HPS4 was generated in collaboration with Zymed Laboratories (South San Francisco, CA), using a GST-fusion protein containing residues 385–594 of human HPS4 for initial immunizations and a polyhistidine-fusion protein containing the same HPS4 fragment for a final boost immunization and subsequent screening of hybridoma clones. Other mAbs were purchased from the indicated vendors: anti-α-tubulin (from Sigma-Aldrich, St. Louis, MO), anti-δ clone 18, anti-early endosome antigen 1 (EEA1) and anti-p47A/μ3A (BD Transduction Laboratories, Lexington, KY), anti-Rab5 (Synaptic Systems, Göttingen, Germany), MEL-5 anti-Tyrp1 (Signet Laboratories, Dedham, MA), B3/25 against human transferrin receptor (TfR; Boehringer Ingelheim, Ridgefield, CT), and FITC-conjugated anti-CD63 and anti-CD71/TfR (Beckman Coulter, Fullerton, CA). The rat hybridoma against mouse TfR was from American Type Culture Collection (Manassas, VA), and the rabbit polyclonal antibodies to PMP70 and biotin were from Zymed Laboratories and Polysciences (Warrington, PA), respectively. Control rabbit IgG was from Southern Biotechnology (Birmingham, AL). Alexa 488-, Cy3-, and horseradish peroxidase (HRP)-conjugated secondary antibodies were from Molecular Probes (Eugene, OR), Jackson ImmunoResearch (West Grove, PA), and GE Healthcare (Waukesha, WI), respectively.

Animals

Breeding pairs of the homozygous mutant strains pearl (B6.C3-*Ap3b1*^{pe}/J), pallid (B6.Cg-*Pldn*^{pa}/J), cocoa (B6.B10-*Hps3*^{coa}/J), and pale ear (B6.C3Fe-*Hps1*^{ep}/J) were kindly provided by Juan S. Bonifacino and Richard T. Swank. C57BL/6J mice were used as wild-type controls. Homozygous pallid/pale ear double mutant mice were described previously (Nazarian *et al.*, 2003). Other homozygous double mutant strains were generated by following a breeding scheme analogous to that described by Meisler *et al.* (1984), which consisted of first obtaining a breeding pair of mice homozygous for one mutation (typically the one causing the less severe coat pigmentation defect) and heterozygous for the other and then identifying among the progeny the homozygous double mutants by either coat color or, if necessary, by test crosses or genotyping.

Cell Culture

Human HeLa, M1, and MNT-1 cell lines and immortalized mouse fibroblasts were obtained and cultured as described (Dell'Angelica *et al.*, 2000). Primary melanocyte cultures were obtained from the epidermis of <3-d-old mice as described by Wu *et al.* (2001). Cells were allowed to attach to gelatin-coated glass coverslips and cultured in TAV medium (Ham's F10 medium supplemented with 10% [vol/vol] horse serum, 2% [vol/vol] fetal calf serum, 100 U/ml penicillin, 0.1 g/l streptomycin, 100 nM dibutyryl-cAMP, 85 nM phorbol myristate 13-acetate) and used for analysis with no passages. In some experiments, cells were incubated for 6 h in TAV medium containing 1 mg/ml leupeptin before fixation.

Small Interference RNA Treatment and Flow Cytometry

M1 fibroblasts were seeded at a density of 3×10^5 cells per 9-cm dish and 12 h and 3 d later were subjected to transfection with small interference RNA (siRNA) duplexes (Dharmacon, Boulder, CO), as described by Motley *et al.* (2003). The following mRNA sequences were selected as targets: GCGAGAAACUGCCUAUUCA and UCUGCAAGCUGACGUAUUU (δ subunit of AP-3), AAGGAUUGCUUUCUCAUUAUU and GAAGGAGUUUGAAAGAGAA (pallidin subunit of BLOC-1), ACGAGAGAGGAUUAAUCUUU (HPS3 subunit of BLOC-2), and GAACUCGACUUGUCUGAAA (HPS4 subunit of BLOC-3). Three days after the second transfection, cells were either fixed for immunofluorescence staining or harvested for biochemical or flow cytometric analyses. Estimation of surface expression levels of CD63 and TfR

by analytical flow cytometry was performed as described (Dell'Angelica *et al.*, 1999b).

Biochemical Procedures

Cytosolic and membrane fractions of HeLa cells or mouse liver were prepared by homogenization in buffer A (20 mM HEPES, pH 7.4, 50 mM KCl, 1 mM dithiothreitol, 1 mM EGTA, 0.5 mM $MgCl_2$, 0.25 mM GTPγS) containing a protease inhibitors mixture (Di Pietro *et al.*, 2004), followed by centrifugation at 15,000× *g* for 10 min and then ultracentrifugation at 120,000× *g* for 90 min, at 4°C. The final membrane pellet was solubilized in 1 ml of buffer A containing protease inhibitors mixture and 1% (wt/vol) Triton X-100. Triton X-100 was added to the cytosolic fraction to match the detergent concentration. Both fractions were cleared by centrifugation for 10 min at 15,000× *g* before immunoprecipitation, which was performed as described above (Di Pietro *et al.*, 2004) except for the use of buffer A in all washing steps.

For membrane association experiments, cytosol and membrane fractions were obtained from fibroblasts by homogenization in buffer B (10 mM HEPES, pH 7.4, 250 mM sucrose, 1 mM dithiothreitol, 1 mM EGTA, 0.5 mM $MgCl_2$, 0.25 mM GTPγS, and protease inhibitors mixture), followed by centrifugation for 5 min at 15,000× *g* and for 15 min at 400,000× *g*, at 4°C.

Immunoblotting was performed as described (Nazarian *et al.*, 2006).

Immunofluorescence Staining and Antibody Internalization Assay

Immunofluorescence staining and internalization of antibodies by cells grown on glass coverslips were performed as described (Dell'Angelica *et al.*, 1997a, 1999b). Samples were examined at room temperature on a Zeiss Axioskop 2 fluorescence microscope (Carl Zeiss, Thornwood, NY), using 40× and 63× objectives for M1 cells and melanocytes, respectively. Digital images were acquired using an Orca-ER digital camera and the AxioVision software (Carl Zeiss), under conditions optimized to prevent signal saturation. To quantify the fluorescence signal of stained melanocytes, digital images of randomly selected cells were saved using coded file names and subsequently were imported into NIH Image 1.62 for analysis by following a "blinded" approach, i.e., by an operator who was unaware of the identity of the samples. For colocalization experiments, stained samples were examined on a Leica TCS SP confocal microscope (Leica, Deerfield, IL).

Electron Microscopy

Internalization of conjugated transferrin (Tf) by MNT-1 cells, fixation and ultracryomicrotomy, whole-mount electron microscopy, immunogold labeling, and analysis were carried out as previously described (Theos *et al.*, 2005), except that Tf-biotin (Invitrogen, Carlsbad, CA) was used instead of Tf-FITC to label endosomes.

Quantification of Hair Melanin

The melanin content of mouse hair samples was estimated by the spectrophotometric method of Ozeki *et al.* (1995), using purified *Sepia officinalis* melanin (Sigma-Aldrich) as a standard.

Statistical Analyses

All statistical tests were performed using GraphPad Prism 4.0 (GraphPad Software, San Diego, CA). Data groups were first analyzed using the D'Agostino and Pearson omnibus normality test and, if no significant deviations from Gaussian distributions were found, subsequently analyzed by one-sample *t* test (for comparison of one data group vs. a reference number) or one-way ANOVA followed by Dunnett's multiple comparison test (for comparison of several data groups vs. a control group). Comparisons between data groups with significant divergence from Gaussian distributions were carried out using the nonparametric Mann-Whitney test.

RESULTS

Physical Interactions Between BLOC-1, BLOC-2, and AP-3

To test for stable physical association between AP-3 and the BLOCs, each endogenous complex was immunoprecipitated under mild, nondenaturing conditions from HeLa cell extracts, and the washed immunoprecipitates were analyzed by immunoblotting using antibodies against representative subunits of each complex (see Table 1 and *Materials and Methods* for further details). Because the AP-3 complex and all BLOCs exist in both soluble and membrane-associated pools (reviewed by Dell'Angelica, 2004), parallel experiments were carried out using cytosolic and solubilized membrane extracts. As shown in Figure 1A, AP-3 and the three BLOCs were detected and immunoprecipitated from each extract. Significantly, BLOC-1 was also detected in BLOC-2 and AP-3 immunoprecipitates obtained from solubilized membrane extracts, but not from those obtained from cytosol (Figure 1A). In addition, BLOC-2 and AP-3 were detected in BLOC-1 immunoprecipitates obtained from solubilized membranes but not from cytosol (Figure 1A). Coimmunoprecipitation of BLOC-2 and AP-3 with BLOC-1 was observed upon immunoprecipitation using antibodies against two different BLOC-1 subunits (Figure 1B). Under these conditions, no specific association between AP-3 and BLOC-2, or between BLOC-3 and any of the other complexes, was detected (Figure 1A). Additional experiments were performed in which BLOC-1 was immunoprecipitated from membrane extracts prepared in the presence of GDP instead of the nonhydrolyzable GTP analog, GTPγS. Although comparable amounts of BLOC-2 were associated to BLOC-1 immunoprecipitates regardless of the guanosine nucleotide used, the association of AP-3 to BLOC-1 was significantly compromised, albeit not completely disrupted, upon substitution of GDP for GTPγS (Figure 1B). Therefore, these results suggest that BLOC-1 interacts, either directly or indirectly, with AP-3 and BLOC-2, and that the two interactions may be differentially regulated.

Next, coimmunoprecipitation experiments were carried out using liver cytosolic and membrane extracts from various mouse strains. Of interest was the analysis of tissue samples from homozygous pallid, cocoa, and pearl mice carrying mutations in genes encoding subunits of BLOC-1, BLOC-2, and AP-3, respectively (Table 1; reviewed by Li *et al.*, 2004). In agreement with the results described above, immunoprecipitation of BLOC-1 from wild-type membrane extracts resulted in coimmunoprecipitation of the AP-3 complex and BLOC-2, and immunoprecipitation of the AP-3 complex or BLOC-2 from the same extracts resulted in coimmunoprecipitation of BLOC-1 (Figure 1C and unpublished data). Again, no coimmunoprecipitation between these complexes was observed using cytosolic extracts. Importantly, no AP-3 was detected upon subjecting extracts prepared from BLOC-1–deficient mice to a "mock" immunoprecipitation using an antibody to a BLOC-1 subunit, and no BLOC-1 was detected upon mock immunoprecipitation of extracts prepared from AP-3–deficient mice using an antibody to AP-3 σ3 (Figure 1C), implying that the observed coimmunoprecipitation was not due to antibody cross-reactivity during the immunoprecipitation step. Similarly, control immunoprecipitations performed in extracts prepared from BLOC-1– or BLOC-2–deficient mice yielded the expected negative results for the BLOC-1·BLOC-2 interaction (unpublished data). Interestingly, the association between BLOC-1 and AP-3 was observed in liver membrane extracts prepared from BLOC-2–deficient mice, and that between BLOC-1 and -2 was observed in extracts prepared from AP-3–deficient mice (Figure 1C and unpublished data). Together, these results provide support to the idea that the interactions between BLOC-1 and BLOC-2 or AP-3 are specific and suggest that BLOC-1 can associate with BLOC-2 independently of AP-3, and likewise, it can associate with AP-3 independently of BLOC-2 function.

Genetic Interactions Between BLOC-1, BLOC-2, and AP-3

As a complementary approach to understand the functional relationships between AP-3 and the BLOCs, we tested for epistatic interactions through generation of homozygous double mutant mice simultaneously deficient in pairs of these protein complexes. Although the coat color phenotype of mice simultaneously deficient in BLOC-1 and BLOC-2 (pallid/cocoa) was virtually indistinguishable from that of

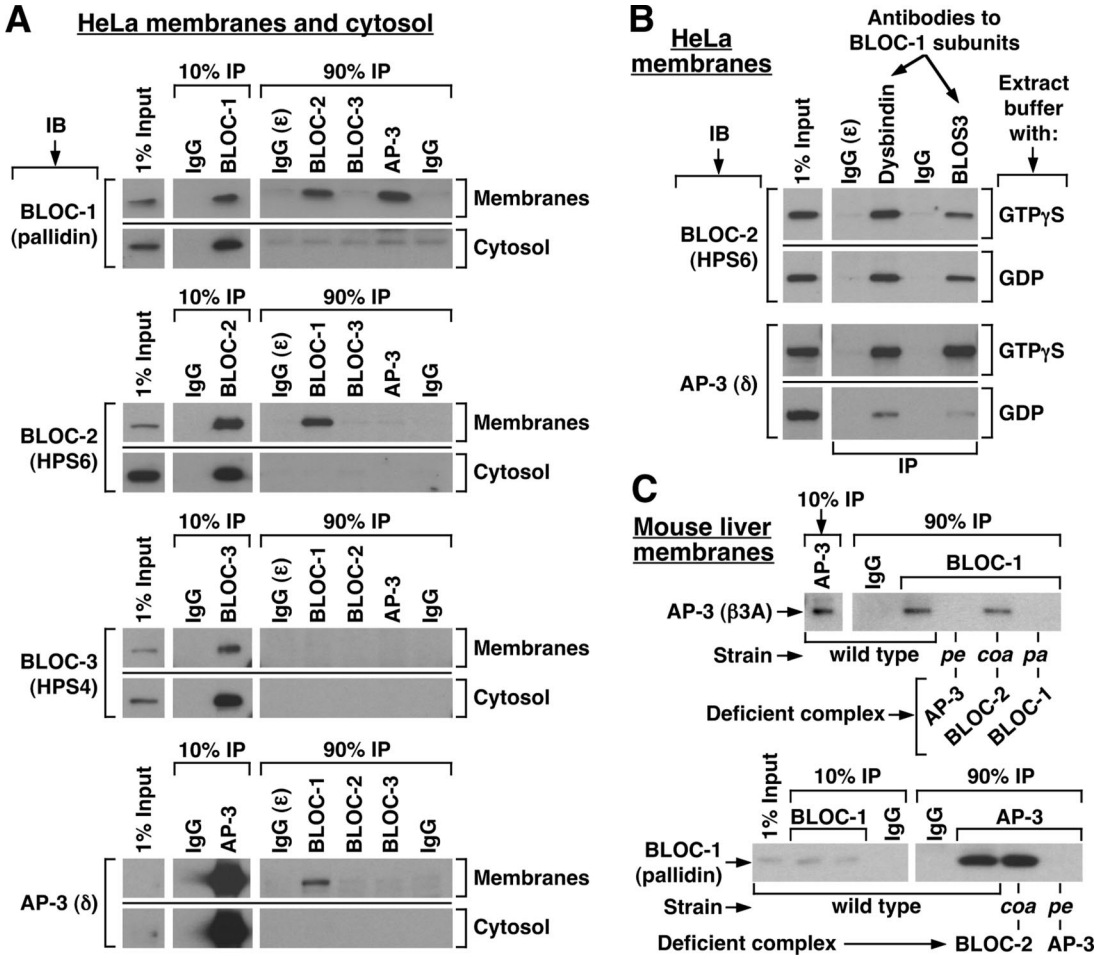

Figure 1. Coimmunoprecipitation of BLOC-1 with BLOC-2 and AP-3. (A) HeLa cells were homogenized in the absence of detergents and presence of GTPγS, and the homogenate was centrifuged to yield cytosolic and membrane fractions. The membrane fraction was solubilized in an excess of buffer containing Triton X-100, and the same detergent was added to the cytosol to match the buffer compositions (see *Materials and Methods*). Both fractions were subjected to immunoprecipitation (IP) using polyclonal antibodies to the dysbindin, HPS6, HPS4, and σ3 subunits of BLOC-1, BLOC-2, BLOC-3, and AP-3, respectively. Irrelevant rabbit IgG, and a polyclonal antibody that fails to recognize its cognate antigen (ε) under nondenaturing conditions, were included as controls. The immunoprecipitates, together with an aliquot of the extracts corresponding to 1% of the material available for IP, were analyzed by immunoblotting (IB) using mAbs to the pallidin, HPS4, and δ subunits of BLOC-1, BLOC-3, and AP-3, respectively, and the HP6d antibody to the HPS6 subunit of BLOC-2. The signal corresponding to 1% of AP-3 δ was detected upon longer exposures than that shown in the figure. (B) HeLa membrane extracts prepared in the presence of GTPγS or GDP were subjected to immunoprecipitation using control IgG or polyclonal antibodies against the dysbindin or BLOS3 subunits of BLOC-1. The immunoprecipitates were analyzed by immunoblotting using antibodies to subunits of BLOC-2 and AP-3. (C) Solubilized liver membranes were prepared in the presence of GTPγS from wild-type mice or from homozygous pallid (*pa*), cocoa (*coa*) and pearl (*pe*) mutant mice deficient in BLOC-1, BLOC-2, and AP-3, respectively. Equivalent total protein amounts of the extracts were subjected to immunoprecipitation using irrelevant rabbit IgG or purified rabbit antibodies to the dysbindin subunit of BLOC-1 or the σ3 subunit of AP-3. The immunoprecipitates were analyzed by immunoblotting using a polyclonal antibody to the β3A subunit of AP-3 and an mAb to the pallidin subunit of BLOC-1.

single mutant mice deficient in BLOC-1, that of mice simultaneously deficient in BLOC-1 and AP-3 (pearl/pallid) was more severe than that of age-matched single mutants (Supplementary Figure 1). In addition, mice simultaneously deficient in AP-3 and BLOC-1 were very difficult to breed as double homozygous, unlike the corresponding single mutants or mice simultaneously deficient in BLOC-1 and BLOC-2 (unpublished data). Strikingly, the coat color phenotype of double mutant mice deficient in AP-3 and BLOC-2 was not only more severe than that of the corresponding single mutants but highly similar to that of BLOC-1–deficient mice (Supplementary Figure 1). The simplest interpretation of these results is that AP-3 and BLOC-2 can function independently of each other and that the impact of BLOC-1 deficiency on pigmentation can be mimicked by simultaneous deficiencies in AP-3 and BLOC-2.

Functional Interactions between BLOC-1, BLOC-2, and AP-3 as Evidenced by Regulation of Membrane Association

As a first step to address the biological significance of the observed interactions between BLOC-1, BLOC-2, and AP-3, we tested whether membrane association of each complex was affected by deficiencies in its interacting partner(s). To this end, cytosolic and membrane fractions were obtained from skin fibroblast lines derived from wild-type and mutant mice, and the relative amounts of each complex in the membrane fraction were estimated by quantitative immu-

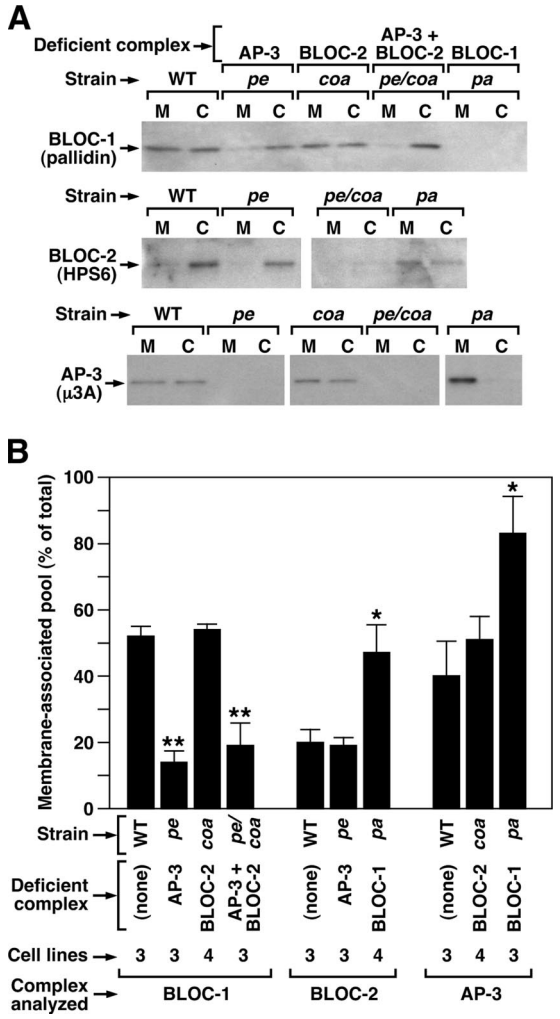

Figure 2. Membrane-associated pools of BLOC-1, BLOC-2 and AP-3 in fibroblasts from mutant mice. (A) Immortalized fibroblasts derived from the skin of C57BL/6J mice (WT), homozygous pallid (*pa*), cocoa (*coa*), and pearl (*pe*) mice deficient in BLOC-1, BLOC-2, and AP-3, respectively, and pearl/cocoa (*pe/coa*) double mutant mice were subjected to a quick homogenization and ultracentrifugation procedure to yield postnuclear membrane (M) and cytosolic (C) fractions (see *Materials and Methods*). Aliquots corresponding to an equivalent cell number were analyzed by immunoblotting using antibodies to the indicated subunits of BLOC-1, BLOC-2, and AP-3. (B) Quantification of the relative amount of each complex that was recovered from the membrane fraction. Bars, means ± SEM of the indicated number of independent fibroblast lines analyzed per strain. For each protein complex, the data groups corresponding to mutant cells were compared with that of wild-type fibroblasts by means of ANOVA followed by Dunnett's test: *$p < 0.05$; **$p < 0.01$.

noblotting. In an attempt to minimize dissociation from membranes during the fractionation procedure, we used a sucrose-containing buffer that had been shown to help stabilize the membrane-associated forms of the three complexes (Dell'Angelica *et al.*, 1997a; Falcón-Pérez *et al.*, 2002; Di Pietro *et al.*, 2004) and we significantly reduced the duration of the ultracentrifugation step (see *Materials and Methods*). Under these conditions, about half of BLOC-1, ~20% of BLOC-2, and ~40% of AP-3 were recovered from the membrane fractions obtained from wild-type mouse fibroblast lines (Figure 2, A and B). Interestingly, the relative amounts of BLOC-1 recovered from membranes were reduced to <20% in AP-3–deficient cells (or in cells simultaneously deficient in AP-3 and BLOC-2), and those of BLOC-2 and AP-3 were increased in BLOC-1–deficient cells (Figure 2). Membranes isolated from BLOC-2–deficient fibroblasts contained relative amounts of BLOC-1 and AP-3 that were comparable to those of wild-type cells, and membranes isolated from AP-3–deficient fibroblasts contained normal amounts of BLOC-2 (Figure 2). In another set of experiments, knockdown of AP-3 expression by siRNA treatment of human M1 cells (see below) resulted in a ~40% decrease in the relative amount of membrane-associated BLOC-1 without affecting the membrane-associated pool of BLOC-2 (unpublished data), thus in agreement with the results obtained using immortalized fibroblasts from mutant mice. As judged from immunofluorescence analysis of fixed/permeabilized fibroblasts, neither the overall distribution of AP-3 nor its degree of colocalization with TfR was noticeably affected by deficiencies in BLOC-1 or -2 (Supplementary Figure 2). Together, these results suggest that AP-3 and BLOC-1 can regulate the membrane association/dissociation of each other, albeit without significantly altering AP-3 distribution, and that BLOC-1 can also regulate membrane association/dissociation of BLOC-2.

Localization of Endogenous BLOC-1 and BLOC-2 to Endosomes

It is well established that AP-3 associates with clathrin-coated buds on early endosome-associated tubules (Dell'Angelica *et al.*, 1998; Peden *et al.*, 2004; Theos *et al.*, 2005), although the existence of a pool of AP-3 associated with pericentriolar endosomal membranes devoid of clathrin has also been noted. In this study, we sought to determine the localization of BLOC-1 by immunoelectron microscopy on ultrathin cryosections of MNT-1, a highly pigmented human melanoma line in which we have characterized the melanosomal maturation stages, the compartments of the endocytic pathway, and the localization of AP-3 (Raposo *et al.*, 2001; Theos *et al.*, 2005). Two of our affinity-purified polyclonal antibodies against BLOC-1 subunits, those against pallidin and dysbindin, resulted in immunogold labeling that was deemed to be specific on the basis of 1) low background labeling in compartments such as nuclei or mitochondria and 2) essentially the same labeling pattern obtained using both antibodies. The antibodies labeled mainly tubulovesicular elements that were distributed throughout the cytoplasm, albeit concentrated in the vicinity of melanosomes and the perinuclear cytoplasmic region that harbors the Golgi apparatus (Figure 3, A–C). Occasional labeling of the melanosomal membrane was also observed. We counted 211 gold particles in randomly selected portions of three independent grids containing ultrathin cryosections of MNT-1 cells labeled with anti-dysbindin. Of them, 148 (70%) were on tubulovesicular elements in the vicinity of the Golgi apparatus and/or pigmented (stage IV) melanosomes, 27 (13%) on vesicles dispersed throughout the cell periphery, 23 (11%) on the melanosomal limiting membrane, 13 (6%) on mitochondria, and none at the plasma membrane or nuclei. This labeling pattern was reminiscent of proteins localized to early endosomes in MNT-1 cells (Raposo *et al.*, 2001; Theos *et al.*, 2005). In fact, BLOC-1 labeling was observed in tubulovesicular elements that also contained internalized Tf-biotin (Figure 3C). We then used the "whole-mount" electron microscopy technique (Stoorvogel *et al.*, 1996) to test for the presence of BLOC-1 on endosomes that had been loaded with internalized Tf-HRP and selectively fixed by cross-linking. Importantly, we observed labeling for endogenous BLOC-1 on cross-linked endosomal tubules that also

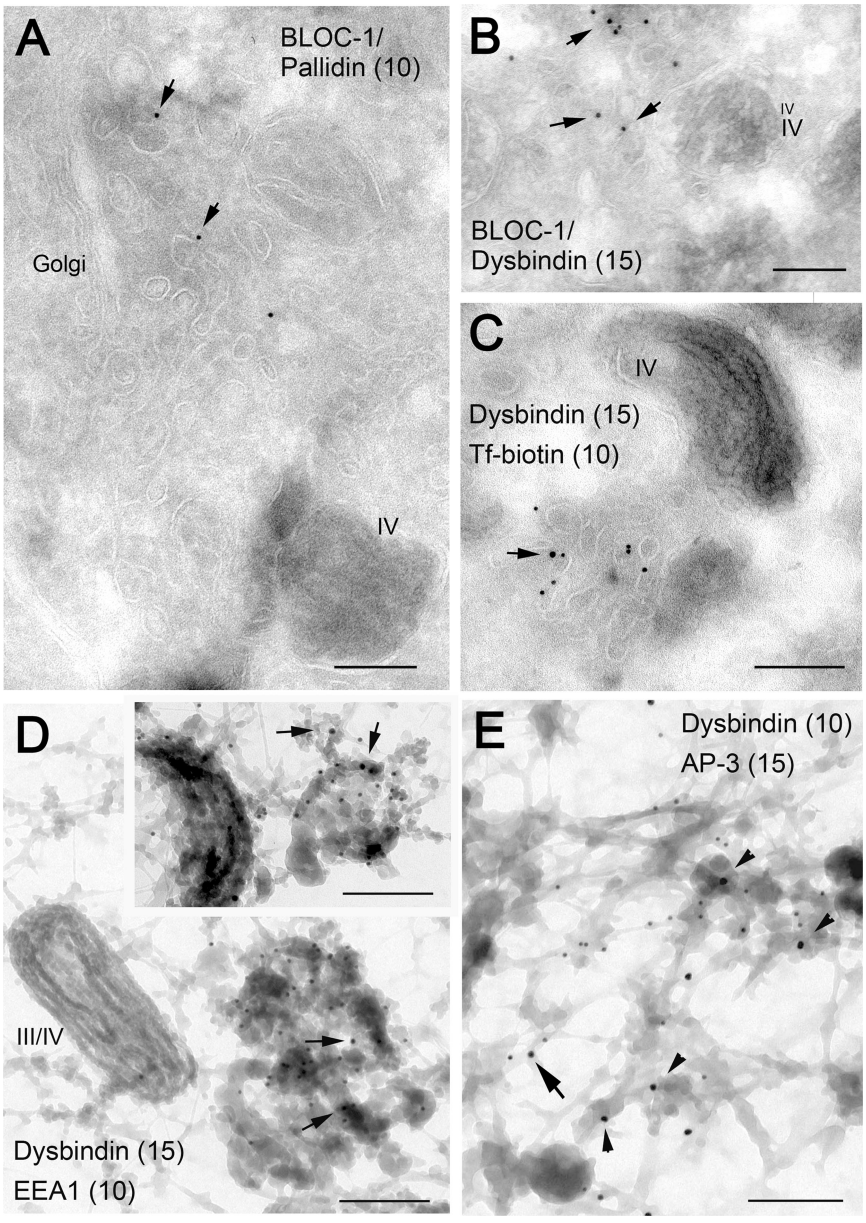

Figure 3. Localization of endogenous BLOC-1 in human MNT-1 cells as determined by immunoelectron microscopy. (A–C) Ultrathin cryosections of MNT1 cells were labeled with polyclonal antibodies against the pallidin (A) or dysbindin (B and C) subunits of BLOC-1 followed by protein A conjugated to 10- or 15-nm gold, as indicated. In C, cells were allowed to internalize Tf-biotin for 45 min before fixation, and Tf-biotin was subsequently detected with anti-biotin followed by protein A gold (10 nm) conjugate. Arrows point at examples of BLOC-1 labeling associated to tubulovesicular membrane profiles, some of them in the vicinity of the Golgi complex or type IV melanosomes. In C, the BLOC-1–positive tubulovesicular structures contained internalized Tf-biotin. (D and E) Immunogold labeling on whole-mounted MNT1 cells in which endosomes were selectively cross-linked with Tf-HRP. (D) BLOC-1 (arrows) was detected on endosomal tubules and occasionally vacuoles (inset) that also contained EEA1. These endosomal elements were often close to pigmented melanosomes (type III or IV). (E) BLOC-1 and AP-3 were detected in the same endosomal network, although relatively less BLOC-1 labeling was observed in AP-3–containing buds (arrowheads) than in tubules, some of which also contained AP-3 (arrow). Bars, 200 nm.

contained EEA1 (Figure 3D) and AP-3 (Figure 3E). Although labeling for BLOC-1 was observed more frequently on endosomal tubules (and, occasionally, vacuoles; see inset in Figure 3D) and that for AP-3 on associated buds, in some instances both complexes were detected in close proximity (e.g., Figure 3E, arrow).

Additional experiments were performed to localize BLOC-2 by immunoelectron microscopy on ultrathin cryosections of MNT-1 cells. Two affinity-purified antibodies against the BLOC-2 subunits, HP3c anti-HPS3, and HP6d anti-HPS6, labeled tubulovesicular elements that, like those labeled for BLOC-1, were often found in the vicinity of the Golgi apparatus or pigmented melanosomes and were accessible to internalized Tf-biotin (Figure 4, A–C). Although for both antibodies the labeling efficiency was low, again it was deemed to be specific based on 1) negligible background labeling of mitochondria and nuclei and 2) basically the same labeling pattern obtained with both antibodies. Labeling for BLOC-2 was best appreciated using the whole-mount technique, which resulted in detection of BLOC-2 associated with endosomal tubules that also contained EEA1 (Figure 4D). The fact that the labeling efficiencies for BLOC-1 and -2 were drastically reduced upon the glutaraldehyde fixation step required for double immunogold labeling experiments (unpublished data) hampered our attempts to test directly for colocalization between these two binding partners.

Taken together, these results indicate that BLOC-1 and -2 localize, at least in part, to early endosomes and their associated tubules.

Knockdown of BLOC-1 from Human Fibroblasts Leads to Cell Surface Accumulation of CD63

The observed interaction between AP-3 and BLOC-1 was surprising given previous data that had suggested that mutant mouse fibroblasts deficient in BLOC-1 do not display a characteristic phenotype of AP-3–deficient cells, i.e., en-

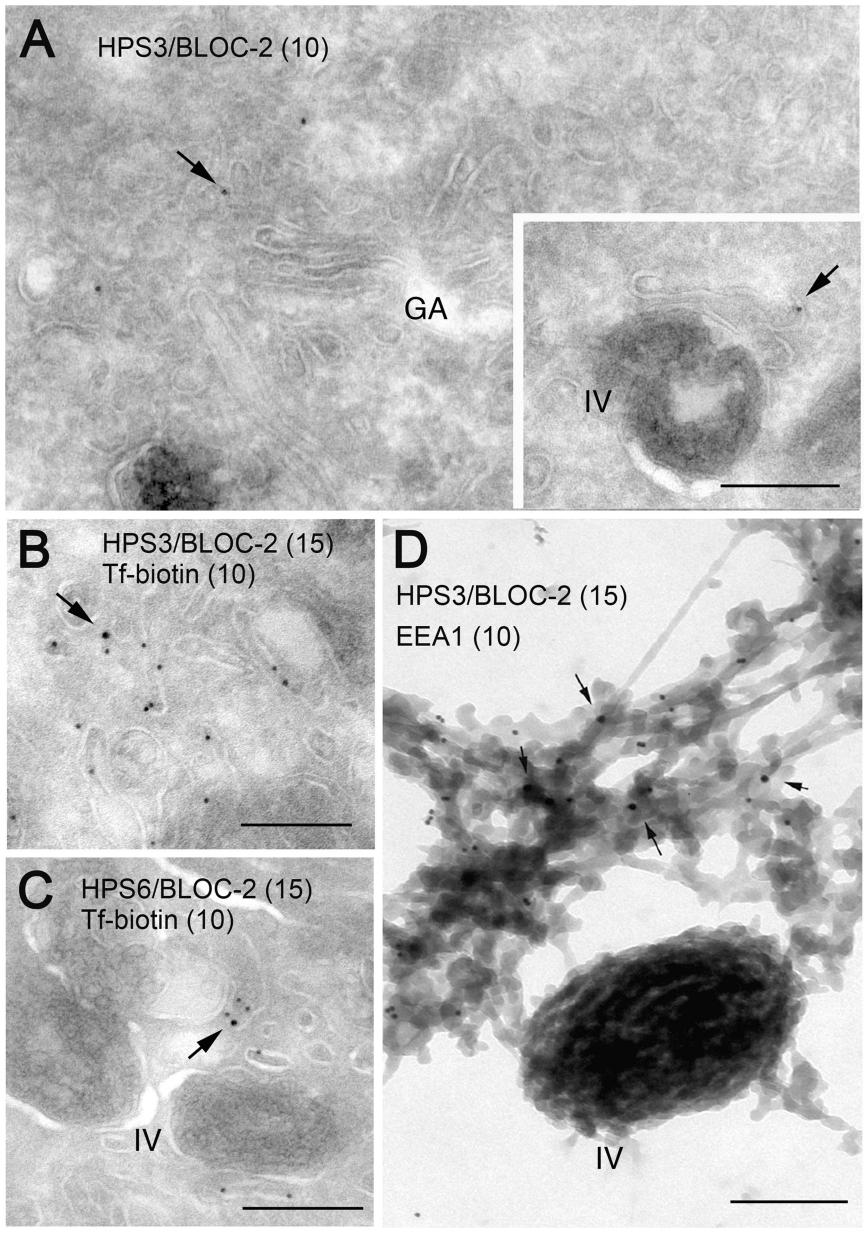

Figure 4. Localization of endogenous BLOC-2 in human MNT-1 cells as determined by immunoelectron microscopy. (A–C) Ultrathin cryosections of MNT-1 cells were labeled with polyclonal antibodies against the HPS3 and HPS6 subunits of BLOC-2, followed by protein A conjugated to 10- or 15-nm gold, as indicated. In B and C, cells were allowed to internalize Tf-biotin for 45 min before fixation, and Tf-biotin was subsequently detected with anti-biotin followed by protein A gold (10 nm) conjugate. BLOC-2 localized to tubulovesicular structures often close to the Golgi complex and/or melanosomes; these structures could be accessed by internalized Tf-biotin. (D) Immunogold labeling for endogenous BLOC-2 and EEA1 on whole-mounted MNT1 cells in which endosomes were selectively cross-linked with Tf-HRP. BLOC-2 (arrows) was detected on EEA1-positive endosomal tubules closely apposed to pigmented (type IV) melanosomes. Bars, 200 nm.

hanced trafficking of LAMP1 through the cell surface (Dell'Angelica *et al.*, 2000; Gwynn *et al.*, 2000; Martina *et al.*, 2003). We first attempted to address this issue by performing flow cytometric analyses of LAMP1 surface levels and internalization, using several independent lines of immortalized fibroblasts derived from mutant mice deficient in each complex. Although our results were suggestive of enhanced LAMP1 trafficking through the surface of mutant fibroblasts deficient in BLOC-1, they failed to reach statistical significance owing to high variability in the results obtained using different cell lines derived from each mouse strain (unpublished data). Similar experiments performed by Salazar *et al.* (2006), however, succeeded in demonstrating enhanced surface levels of endogenous LAMP1 is BLOC-1–deficient mouse fibroblasts, notwithstanding the variability between cell lines. Here, we adopted an alternative experimental approach that was based on acute knockdown of BLOC-1 expression in the human M1 fibroblastoid cell line by siRNA, followed by analysis of the endogenous CD63/LAMP3 protein by indirect immunofluorescence and flow cytometry. Among the advantages of this approach were the use of a single immortalized cell line analyzed in parallel upon different siRNA treatments, as opposed to a comparison between independent mutant cell lines, and the use of endogenous CD63 as a marker for AP-3–dependent trafficking, which facilitated quantitative analyses with improved signal-to-noise ratio (Dell'Angelica *et al.*, 1999b; Janvier and Bonifacino, 2005). We identified two independent siRNA duplexes that were able to significantly knockdown expression of BLOC-1, two for efficient knockdown of AP-3, and one siRNA duplex to knockdown expression of each of BLOC-2 and -3 (Figure 5A). In agreement with published data (Janvier and Bonifacino, 2005), knockdown of AP-3 led to a significant accumulation of CD63 at the cell surface, which was readily detected by indirect immunofluorescence (Figure 5D) and flow cytometry (Figure 5E). Interestingly, knockdown of BLOC-1 with either siRNA duplex elicited a similar effect, albeit to a lesser extent, as judged by both

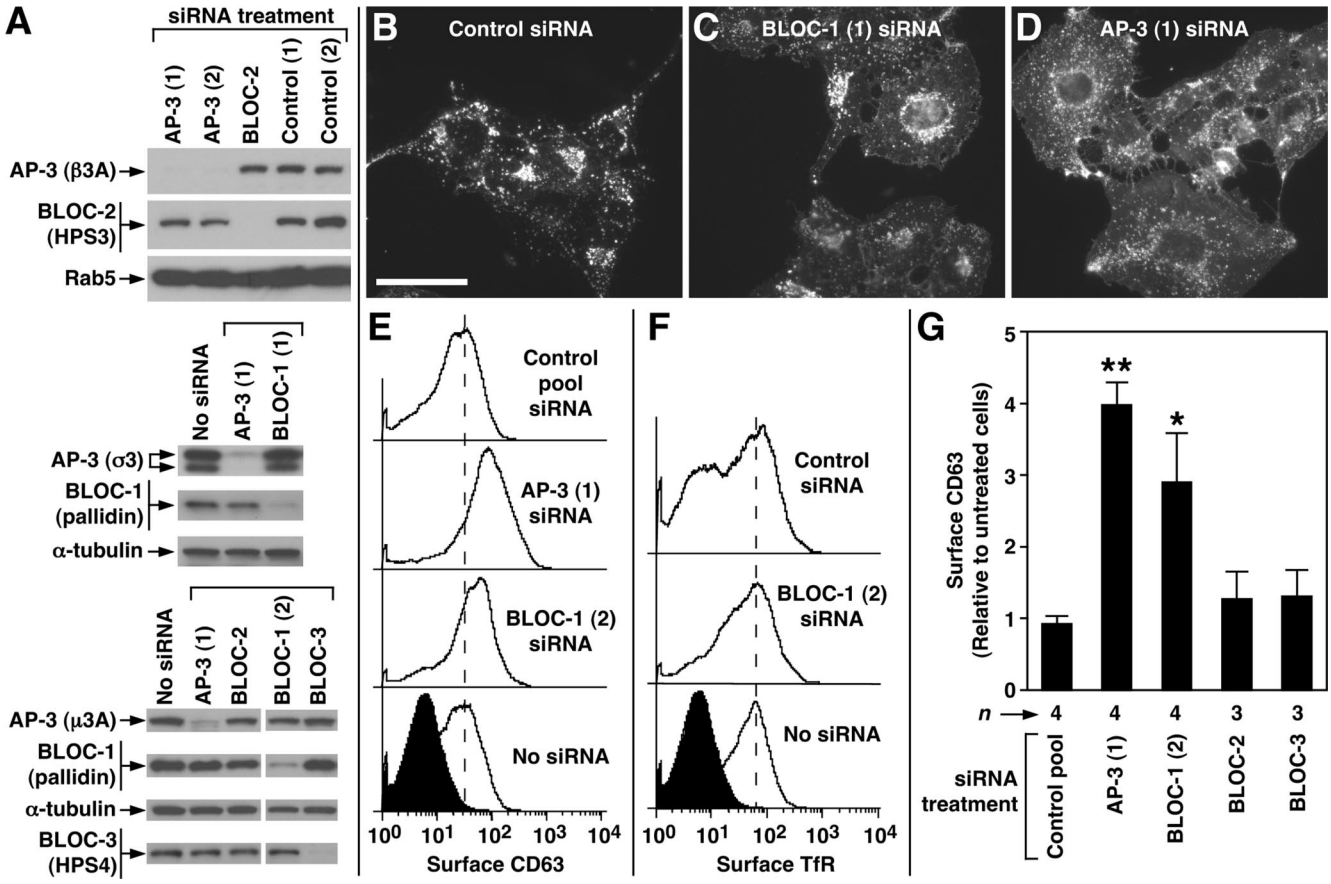

Figure 5. Knockdown of AP-3 and BLOC-1 in human fibroblasts elicits surface accumulation of CD63. (A) Human M1 fibroblasts were either mock-treated (*No siRNA*) or treated with siRNA duplexes to target the δ subunit of AP-3, the pallidin subunit of BLOC-1, the HPS6 subunit of BLOC-2, the HPS4 subunit of BLOC-3, or to irrelevant targets (*control*). Whole-cell lysates were prepared and analyzed by immunoblotting using antibodies to the indicated proteins. (B–D) Representative immunofluorescence images of M1 fibroblasts treated with an irrelevant siRNA duplex (B) or with specific siRNA duplexes to knockdown expression of BLOC-1 (C) or AP-3 (D), followed by fixation/permeabilization and staining using an mAb to endogenous CD63. Notice the relatively higher levels of CD63 associated with the plasma membrane of BLOC-1– or AP-3–deficient cells, as revealed by a higher intensity of homogeneous "haze" signal amid the punctuate staining corresponding to intracellular CD63. Bar, 50 μm. (E and F) Distributions of the surface levels of CD63 (E) and TfR (F) in mock-treated (*No siRNA*) and siRNA-treated M1 fibroblasts, as determined by immunostaining of nonpermeabilized cells with FITC-conjugated antibodies followed by flow cytometry. The filled distributions correspond to cells immunostained using an irrelevant FITC-conjugated antibody (against goat IgG). Dashed vertical lines are placed at arbitrary positions to facilitate the visual comparison of the distributions. (G) Statistical analysis of results obtained in independent experiments in which M1 cells were treated with a control siRNA pool or with specific siRNA duplexes to target AP-3 and each of the BLOCs, followed by quantification of CD63 surface levels by flow cytometry. Values are expressed as the ratio between the mean CD63 fluorescence signal of siRNA-treated cells and that of untreated cells, which were analyzed in parallel in each experiment. Bars, means ± SEM of the indicated numbers of independent experiments (n). One-way ANOVA followed by Dunnett's test of each group versus treatment with control pool siRNA: *$p < 0.05$; **$p < 0.01$.

methods (Figure 5, C, E, and G). On the other hand, the surface levels of CD63 were not noticeably affected upon knockdown of BLOC-2 or -3 (Figure 5G). Like in AP-3–deficient cells, the surface levels of TfR were not affected by knockdown of BLOC-1 (Figure 5F). These observations suggest that BLOC-1 plays a role in the trafficking of CD63/LAMP3, a well-known AP-3 cargo.

Abnormal Tyrp1 Trafficking and Steady State Levels in Melanocytes Deficient in BLOC-1, BLOC-2, and AP-3

In a recent study, we have found that melanocytes deficient in BLOC-1 display abnormal accumulation of Tyrp1 in early endosomes (positive for EEA1, syntaxin 13, and internalized Tf), with increases in the amounts of Tyrp1 trafficking to the plasma membrane and undergoing internalization (S.R.G. Setty, M. Starcevic, D. Tenza, S. T. Truschel, E. Chou, A. C. Theos, E. V. Sviderskaya, M. L. Lamoreux, D. C. Bennett, E. C. Dell'Angelica, G. Raposo, and M. S. Marks, unpublished results). Here, we sought to determine the extent to which BLOC-2 and AP-3 contribute to the role of BLOC-1 in trafficking of Tyrp1 to melanosomes. To this end, we have obtained and analyzed primary skin melanocyte cultures deficient in AP-3 and/or the BLOCs. Our decision to use primary melanocytes endogenously expressing Tyrp1 was aimed at avoiding concerns associated with the use of transformed melanocyte lines or with experiments involving expression of Tyrp1 by transfection, although the yields of primary melanocytes were not sufficient to allow flow cytometric or biochemical analyses. Here, live cells were allowed to simultaneously internalize antibodies to the luminal domains of Tyrp1 and TfR, and they were subsequently fixed/permeabilized and incubated with species-specific

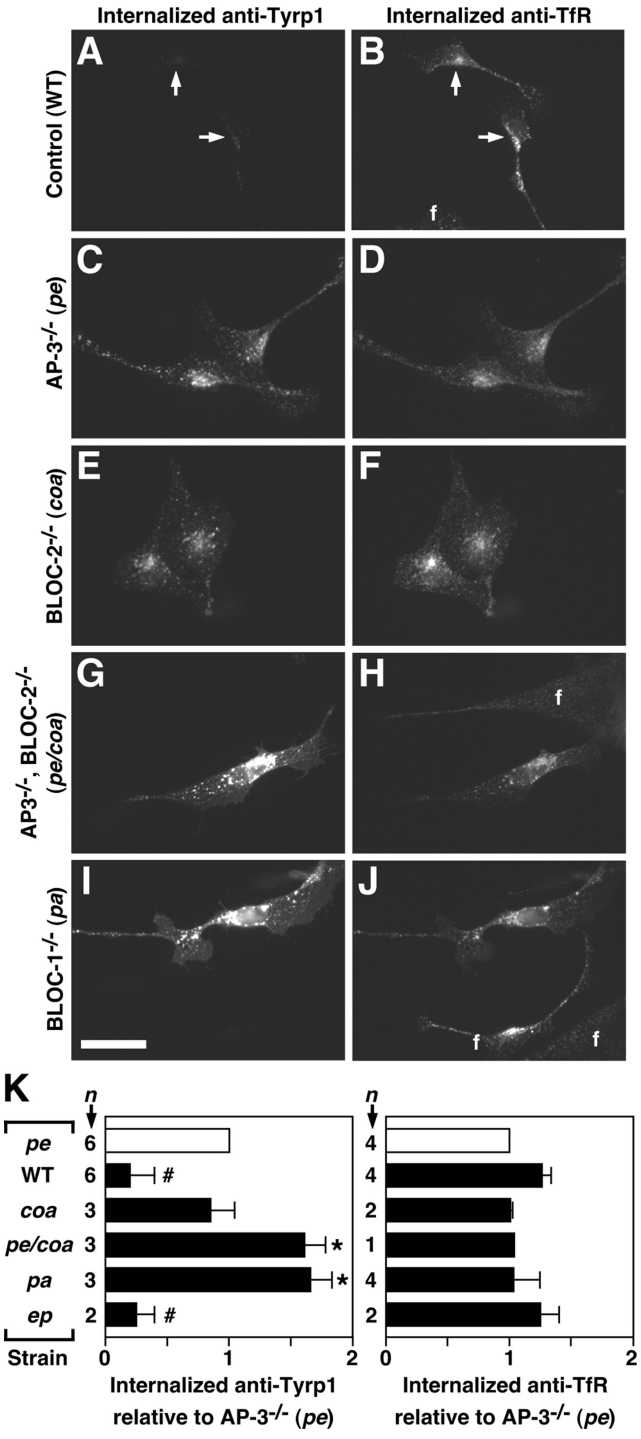

Figure 6. Enhanced flux of Tyrp1 internalization in primary skin melanocytes from mutant mice deficient in AP-3, BLOC-1 or BLOC-2. (A–K) Skin melanocytes were cultured from mice of the control C57BL/6J strain (WT), the homozygous mutant strains pearl (*pe*), pallid (*pa*), cocoa (*coa*), and pale ear (*ep*) deficient in AP-3, BLOC-1, BLOC-2, and BLOC-3, respectively, or from the *pe/coa* double mutant strain. Live cells were allowed to internalize a mouse mAb to Tyrp1 together with a rat mAb to TfR for 20 min at 37°C and subsequently were fixed/permeabilized and incubated with Cy3-conjugated anti-mouse IgG and Alexa-488–conjugated anti-rat IgG. Digital fluorescence microscopy images of internalized anti-Tyrp1 (A, C, E, G, and I) and anti-TfR (B, D, F, H, and J) were acquired and processed under identical conditions for each antibody. Bar, 25 μm. Contaminating fibroblasts (f) were present in the cultures and, as expected, internalized anti-TfR but not anti-Tyrp1. (K) The relative amounts of internalized anti-Tyrp1 and anti-TfR were estimated for each strain as the average fluorescence intensity per cell of 24–62 randomly selected melanocytes per independent culture and normalized to the average value obtained for AP-3–deficient melanocytes (□) analyzed in parallel. Solid bars represent means ± SD of the indicated number of independent cultures per strain. One-sample *t* test: # and *, lower and higher, respectively, than the reference value of 1 set for AP-3–deficient melanocytes, with $p < 0.05$.

secondary antibodies to reveal both primary antibodies internalized by the same cell. A strong signal corresponding to internalized anti-Tyrp1 (as well as some antibody bound to Tyrp1 at the cell surface) was observed in BLOC-1-deficient melanocytes (Figure 6I) under conditions in which the corresponding signal was barely detectable in wild-type melanocytes (Figure 6A). In contrast, both wild-type and mutant cells displayed comparable amounts of internalized anti-TfR (Figure 6, B and J). Interestingly, internalization of anti-Tyrp1, but not of TfR, was also enhanced in melanocytes from AP-3– or BLOC-2–deficient mice (Figure 6, C–F). To test whether the observed differences were statistically significant, several independent primary culture preparations were analyzed for each strain. The average fluorescence signal per cell for each preparation of each strain were determined using a "blinded" approach, averaged and normalized to that of AP-3–deficient melanocytes analyzed in parallel (we chose to normalize the data to that of AP-3–deficient melanocytes owing to the low signal of anti-Tyrp1 obtained for wild-type melanocytes). The results of these analyses are shown in Figure 6K. Relative to AP-3–deficient melanocytes, the amounts of internalized Tyrp1 were significantly lower in wild-type and BLOC-3–deficient melanocytes, comparable in BLOC-2–deficient melanocytes, and significantly higher in BLOC-1–deficient melanocytes. In contrast, the amounts of internalized anti-TfR were either comparable or modestly increased in wild-type and BLOC-3–deficient melanocytes, relative to those of AP-3 mutant melanocytes. Of note was the phenotype of melanocytes cultured from homozygous AP-3/BLOC-2 double mutant mice (*pe/coa*), which was strikingly similar to that of BLOC-1–deficient melanocytes (Figure 6, G–K).

Possible caveats to the antibody internalization assay were considered. First, the possibility that differences in mean fluorescence intensity per cell could be secondary to differences in cell size was ruled out through comparison of areas of the melanocyte images used for quantification (unpublished data). Second, the possibility that the observed increases in surface/internalized Tyrp1 could be secondary to increases in total Tyrp1 expression levels was addressed by immunofluorescence staining of fixed/permeabilized cells. Surprisingly, not only was the immunofluorescence signal corresponding to endogenous Tyrp1 not higher in mutant melanocytes, compared with that of wild-type melanocytes, but it was dramatically reduced (Figure 7, A–F). The differences were statistically significant, as determined by "blinded" analysis of independent primary melanocyte preparations for each strain (Figure 7G). Again, the phenotype was more severe in melanocytes deficient in BLOC-1 or simultaneously deficient in AP-3 and BLOC-2 (*pe/coa*) than in cells deficient in either AP-3 or BLOC-2 alone. As expected, the immunofluorescence signal of an irrelevant membrane protein, PMP70, was not reduced in mutant melanocytes relative to wild-type melanocytes (Figure 7G). We reasoned that missorting to lysosomes could in part contrib-

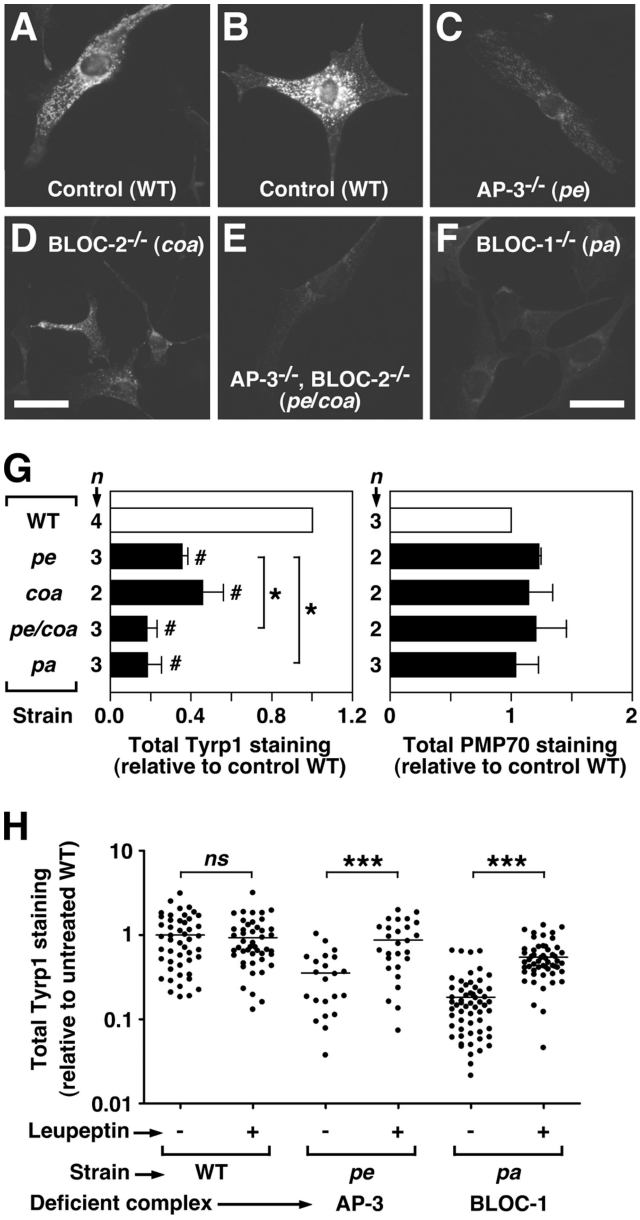

Figure 7. Decreased steady-state Tyrp1 protein levels in primary skin melanocytes from mutant mice deficient in AP-3, BLOC-1, or BLOC-2. Skin melanocytes were cultured from mice of the control C57BL/6J strain (WT), the homozygous mutant strains pearl (*pe*), pallid (*pa*), and cocoa (*coa*) deficient in AP-3, BLOC-1, and BLOC-2 respectively, or from the *pe/coa* double mutant strain. Cells were fixed/permeablized and stained using a mouse mAb to Tyrp1 together with a rabbit polyclonal antibody to peroxisomal membrane protein 70 (PMP70), followed by Cy3-conjugated anti-mouse IgG and Alexa-488–conjugated anti-rabbit IgG. (A–F) Representative fluorescence microscopy images of anti-Tyrp1 staining, which were acquired and processed under identical conditions. Bar, 25 μm. (G) The relative amounts of anti-Tyrp1 and anti-PMP70 staining were estimated as the average fluorescence intensity per cell of 22–59 randomly selected melanocytes per independent culture for each strain and normalized to the average value obtained for wild-type melanocytes (□) analyzed in parallel. Solid bars represent means ± SD of the indicated number of independent cultures per strain. $^{\#}p < 0.05$, different from the reference value of 1 set for wild-type melanocytes (one-sample *t* test). $^{*}p < 0.05$, different from AP-3–deficient (*pe*) melanocytes (ANOVA followed by Dunnett's test). (H) Cultured wild-type, pearl (*pe*), and pallid (*pa*) melanocytes were divided into two aliquots and incubated in medium alone (−) or medium containing 1 mg/ml leupeptin (+) for 6 h before fixation/permeabilization, followed by immunofluorescence staining and image analysis. Data points represent the Tyrp1 staining signal per cell of randomly selected melanocytes in each sample, normalized to the average signal obtained for wild-type melanocytes not treated with leupeptin. Horizontal lines represent mean values. Mann-Whitney test of each group of leupeptin-treated versus untreated melanocytes: ns, not significant; $^{***}p < 0.001$.

ute to the reduced steady state levels of Tyrp1, especially if the lumenal epitope recognized by the MEL-5 mAb was sensitive to lysosomal degradation. To address this point, primary cultures of wild-type, AP-3–deficient, and BLOC-1–deficient melanocytes were divided into two aliquots: one aliquot was incubated with medium containing the lysosomal protease inhibitor, leupeptin, and the other with medium alone, for 6 h before cell fixation and immunofluorescence staining. Fluorescence images of randomly selected cells were acquired under identical conditions and quantified. As shown in Figure 7H, treatment with leupeptin led to relatively higher Tyrp1 staining intensities in both AP-3– and BLOC-1–deficient melanocytes, but not in wild-type melanocytes. Moreover, the Tyrp1 staining of leupeptin-treated, AP-3–deficient melanocytes was comparable to that of wild-type melanocytes (Figure 7H). Similar results were obtained in another experiment using an independent preparation of AP-3–deficient melanocytes as well as BLOC-2–deficient melanocytes ($p < 0.001$, leupeptin-treated vs. control cells).

Taken together, these results suggest that the endosomal trafficking of Tyrp1 is abnormal in melanocytes deficient in AP-3 or BLOC-2, and even more so in melanocytes deficient in BLOC-1 or simultaneously deficient in AP-3 and BLOC-2.

DISCUSSION

The finding that HPS can arise from mutations in the gene encoding the β3A subunit of AP-3 (Dell'Angelica *et al.*, 1999b) had raised the expectation that other genes associated with this disease would encode components of the AP-3–dependent trafficking machinery. However, evidence for a functional link between AP-3 and the protein complexes containing the products of other *HPS* genes, i.e., the BLOCs, has remained elusive (reviewed by Li *et al.*, 2004; Wei, 2006). In this study, we demonstrate that BLOC-1 interacts physically and cooperates with AP-3 and BLOC-2 to facilitate protein trafficking on endosomes.

We show that endogenous BLOC-1 from human cells or mouse tissue can associate with BLOC-2 or AP-3 into macromolecular assemblies that are stable enough to allow detection by coimmunoprecipitation. Stability of the BLOC-1·AP-3 assembly in vitro was dependent on the presence of GTPγS, suggesting the possible involvement of a GTPase in regulating its association/dissociation. It is likely that we (Falcón-Pérez *et al.*, 2002) and others (Moriyama and Bonifacino, 2002) had previously failed to detect the BLOC-1·AP-3 interaction owing to enhanced dissociation in the absence of GTPγS and presence of salt at high concentrations. Our results imply that interactions between BLOC-1 and either BLOC-2 or AP-3 occur on membranes and, in turn, regulate their membrane association/dissociation. Thus, the pool of membrane associated BLOC-1 was reduced in cells deficient in AP-3, whereas those of AP-3 and BLOC-2 were increased in BLOC-1–deficient cells. The simplest interpretation of these results is that AP-3 facilitates membrane recruitment of BLOC-1, which in turn facilitates

AP-3 (and BLOC-2) dissociation. We speculate that BLOC-1 might play a role downstream of AP-3–mediated vesicle formation, such as serving as a tethering factor, which would be also consistent with our finding of a small pool of BLOC-1 associated with the melanosomal membrane as well as previous reports on the ability of BLOC-1 subunits to bind SNARE proteins (e.g., Huang *et al.*, 1999) and the detection of BLOC-1 subunits in AP-3–derived vesicles isolated from PC12 cells (Salazar *et al.*, 2005b, 2006). Alternatively, AP-3 and BLOC-1 might interact to delineate the boundaries of two membrane domains on early endosomes, such that a deficiency in one complex could have an indirect impact on the membrane-associated pool of the other. Despite the localization of both complexes to early endosome-associated tubules, it is noteworthy that not much BLOC-1 immunoreactivity was detected on AP-3–containing buds emanating from these tubules. Here, several possible explanations must be considered, namely, 1) that BLOC-1 could be associated with AP-3–containing buds but with epitopes not accessible for recognition by our antibodies upon whole-mount immunoelectron microscopy, 2) that BLOC-1 could be recruited to AP-3 vesicles only subsequently to budding, and 3) that BLOC-1 could be associated with a pool of AP-3–positive, clathrin-negative endosomal membrane profiles that had previously been noted in MNT-1 and other cell types (Peden *et al.*, 2004; Theos *et al.*, 2005).

In support of the idea that the BLOC-1·AP-3 interaction is biologically significant, we show that knockdown of BLOC-1 expression in human fibroblasts elicits surface accumulation of a well-established AP-3 cargo, CD63, and not TfR, and that melanocytes deficient in AP-3 display abnormal trafficking of Tyrp1, which is severely affected in BLOC-1–deficient melanocytes. The conclusion that Tyrp1 trafficking is not entirely independent of AP-3 function is at variance with that of a previous article by Huizing *et al.* (2001), although we note that the immunofluorescence staining shown in that article for Tyrp1 in AP-3–deficient human melanocytes appears to be significantly less intense than in normal melanocytes, thus in agreement with our results. We also demonstrate that trafficking of Tyrp1, but apparently not CD63, also depends in part on BLOC-2 function. Together, our biochemical, genetic, and functional data are most consistent with a model in which BLOC-1 functions in two apparently distinct mechanisms for trafficking of Tyrp1 from endosomes to melanosomes, one of them dependent on AP-3 and the other on BLOC-2 (Figure 8). Such a model provides a satisfactory explanation for our observation that the Tyrp1 trafficking phenotype of BLOC-1–deficient melanocytes is more severe than those of cells deficient in either BLOC-2 or AP-3 but it can be mimicked by the combined deficiency in the last two complexes. This observation is in turn consistent with our results on the coat color phenotypes of double mutant mice. The fact that AP-3 can still function independently of BLOC-1, as suggested by the more severe phenotype of AP-3/BLOC-1 double mutant mice compared with that of BLOC-1–deficient mice, indicates the existence of AP-3–dependent trafficking mechanisms that are independent of BLOC-1, of which tyrosinase (Huizing *et al.*, 2001; Theos *et al.*, 2005) is a likely cargo (Figure 8). The model implies that defective function in any of these complexes would result in missorting of Tyrp1 from early endosomes to the plasma membrane, thus explaining the observed increase in anti-Tyrp1 internalized over a time period, as well as possible missorting into the degradative pathway in lysosomes, consistent with the observed decrease in steady state Tyrp1 levels and its rescue upon leupeptin treatment. Interestingly, the idea that AP-3 deficiency can lead to missorting of some of its cargo into intralumenal vesicles for degradation in lysosomes would provide an attractive explanation to previous reports of decreased immunoreactivity of zinc transporter 3 (Kantheti *et al.*, 1998) and vesicular γ-aminobutyric acid transporter (Nakatsu *et al.*, 2004) in AP-3–deficient mouse brain.

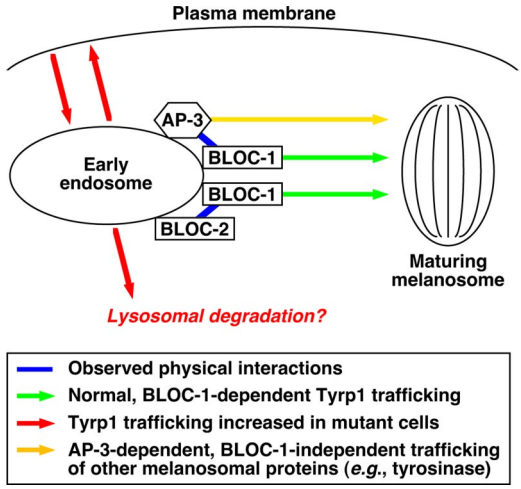

Figure 8. Schematic model of how BLOC-1, BLOC-2, and AP-3 may cooperate to facilitate Tyrp1 trafficking from endosomes to melanosomes. See the text for details.

The observed physical and functional interaction between AP-3 and BLOC-1 may be relevant to the proposed involvement of the latter in the pathogenesis of schizophrenia. Specifically, several independent studies have obtained evidence for association between haplotypes within the gene encoding the dysbindin subunit of BLOC-1 and an increased risk of developing the disease (reviewed by Harrison and Weinberger, 2005; Norton *et al.*, 2006), and recent work has suggested that the *MUTED* gene—encoding the muted subunit of the same complex—may likewise be a schizophrenia susceptibility gene (Straub *et al.*, 2005). Although the mechanisms by which genetic variations in genes encoding BLOC-1 subunits contribute to the risk of schizophrenia remains obscure, circumstantial evidence has suggested a possible functional link with vesicular glutamate transporter 1 (Talbot *et al.*, 2004). Intriguingly, the trafficking of this vesicular neurotransmitter transporter has been shown to depend in part on AP-3 function (Salazar *et al.*, 2005a). Hence, the possibility that BLOC-1 may interact with AP-3 to regulate the trafficking of vesicular glutamate transporter 1 (or of other relevant transporters such as vesicular γ-aminobutyric acid transporter; see Nakatsu *et al.*, 2004) warrants future investigation.

ACKNOWLEDGMENTS

We thank Juan S. Bonifacino, Michael J. Clague, Andrew A. Peden, and Richard T. Swank for their generous gifts of reagents, and Juan S. Bonifacino and the members of Dell'Angelica's laboratory for critical reading of the manuscript. This work was supported by National Institutes of Health (NIH) grants HL068117 and EY015143 (E.C.D.) and EY015625 (M.S.M), and by Centre National de la Recherche Scientifique and Institut Curie grants (G.R.). Flow cytometry was performed in the UCLA Jonsson Comprehensive Cancer Center and Center for AIDS Research Flow Cytometry Core Facility, which is supported by NIH Grants CA16042 and AI28697.

REFERENCES

Clark, R. H., Stinchcombe, J. C., Day, A., Blott, E., Booth, S., Bossi, G., Hamblin, T., Davis, E. G., and Griffiths, G. M. (2003). Adaptor protein 3-de-

pendent microtubule-mediated movement of lytic granules to the immunological synapse. Nat. Immunol. *4*, 1111–1120.

Dell'Angelica, E. C., Ohno, H., Ooi, C. E., Rabinovich, E., Roche, K. W., and Bonifacino, J. S. (1997a). AP-3, an adaptor-like protein complex with ubiquitous expression. EMBO J. *16*, 917–928.

Dell'Angelica, E. C., Ooi, C. E., and Bonifacino, J. S. (1997b). β3a-adaptin, a subunit of the adaptor-like complex AP-3. J. Biol. Chem. *272*, 15078–15084.

Dell'Angelica, E. C., Klumperman, J., Stoorvogel, W., and Bonifacino, J. S. (1998). Association of the AP-3 adaptor complex with clathrin. Science *280*, 431–434.

Dell'Angelica, E. C., Mullins, C., and Bonifacino, J. S. (1999a). AP-4, a novel protein complex related to clathrin adaptors. J. Biol. Chem. *274*, 7278–7285.

Dell'Angelica, E. C., Shotelersuk, V., Aguilar, R. C., Gahl, W. A., and Bonifacino, J. S. (1999b). Altered trafficking of lysosomal proteins in Hermansky-Pudlak syndrome due to mutations in the β3A subunit of the AP-3 adaptor. Mol. Cell *3*, 11–21.

Dell'Angelica, E. C., Aguilar, R. C., Wolins, N., Hazelwood, S., Gahl, W. A., and Bonifacino, J. S. (2000). Molecular characterization of the protein encoded by the Hermansky-Pudlak syndrome type 1 gene. J. Biol. Chem. *275*, 1300–1306.

Dell'Angelica, E. C. (2004). The building BLOC(k)s of lysosomes and related organelles. Curr. Opin. Cell Biol. *16*, 458–464.

Di Pietro, S. M., Falcón-Pérez, J. M., and Dell'Angelica, E. C. (2004). Characterization of BLOC-2, a complex containing the Hermansky-Pudlak syndrome proteins HPS3, HPS5 and HPS6. Traffic *5*, 276–283.

Falcón-Pérez, J. M., Starcevic, M., Gautam, R., and Dell'Angelica, E. C. (2002). BLOC-1, a novel complex containing the pallidin and muted proteins involved in the biogenesis of melanosomes and platelet dense granules. J. Biol. Chem. *277*, 28191–28199.

Faúndez, V., Horng, J.-T., and Kelly, R. B. (1998). A function for the AP3 coat complex in synaptic vesicle formation from endosomes. Cell *93*, 423–432.

Feng, L., Novak, E. K., Hartnell, L. M., Bonifacino, J. S., Collinson, L. M., and Swank, R. T. (2002). The Hermansky-Pudlak syndrome 1 (HPS1) and HPS2 genes independently contribute to the production and function of platelet dense granules, melanosomes, and lysosomes. Blood *99*, 1651–1658.

Fontana, S., *et al.* (2006). Innate immunity defects in Hermansky-Pudlak type 2 syndrome. Blood *107*, 4857–4864.

Gautam, R., Chintala, S., Li, W., Zhang, Q., Tan, J., Novak, E. K., Di Pietro, S. M., Dell'Angelica, E. C., and Swank, R. T. (2004). The Hermansky-Pudlak syndrome 3 (cocoa) protein is a component of the biogenesis of lysosome-related organelles complex-2 (BLOC-2). J. Biol. Chem. *279*, 12935–12942.

Gwynn, B., *et al.* (2000). Defects in the cappuccino (*cno*) gene on mouse chromosome 5 and human 4p cause Hermansky-Pudlak syndrome by an AP-3-independent mechanism. Blood *96*, 4227–4235.

Gruenberg, J., and Stenmark, H. (2004). The biogenesis of multivesicular endosomes. Nat. Rev. Mol. Cell Biol. *5*, 317–323.

Harrison, P. J., and Weinberger, D. R. (2005). Schizophrenia genes, gene expression, and neuropathology: on the matter of their convergence. Mol. Psychiatry *10*, 40–68.

Huang, L., Kuo, Y.-M., and Gitschier, J. (1999). The pallid gene encodes a novel, syntaxin 13-interacting protein involved in platelet storage pool deficiency. Nat. Genet. *23*, 329–332.

Huizing, M., Sarangarajan, R., Strovel, E., Zhao, Y., Gahl, W. A., and Boissy, R. E. (2001). AP-3 mediates tyrosinase but not TRP-1 trafficking in human melanocytes. Mol. Biol. Cell *12*, 2075–2085.

Janvier, K., and Bonifacino, J. S. (2005). Role of the endocytic machinery in the sorting of lysosome-associated membrane proteins. Mol. Biol. Cell *16*, 4231–4242.

Kantheti, P., *et al.* (1998). Mutations in AP-3 δ in the *mocha* mouse links endosomal transport to storage deficiency in platelets, melanosomes, and synaptic vesicles. Neuron *21*, 111–122.

Li, W., Rusiniak, M. E., Chintala, S., Gautam, R., Novak, E. K., and Swank, R. T. (2004). Murine Hermansky-Pudlak syndrome genes: regulators of lysosome-related organelles. Bioessays *26*, 616–628.

Martina, J. A., Moriyama, K., and Bonifacino, J. S. (2003). BLOC-3, a protein complex containing the Hermansky-Pudlak syndrome gene products HPS1 and HPS4. J. Biol. Chem. *278*, 29376–29384.

Meisler, M. H., Wanner, L., and Strahler, J. (1984). Pigmentation and lysosomal phenotypes in mice doubly homozygous for both light-ear and pale-ear mutant alleles. J. Hered. *75*, 103–106.

Mills, I. G., Jones, A. T., and Clague, M. J. (1998). Involvement of the endosomal autoantigen EEA1 in homotypic fusion of early endosomes. Curr. Biol. *8*, 881–884.

Moriyama, K., and Bonifacino, J. S. (2002). Pallidin is a component of a multi-protein complex involved in the biogenesis of lysosome-related organelles. Traffic *3*, 666–677.

Motley, A., Bright, N. A., Seaman, M. N. J., and Robinson, M. S. (2003). Clathrin-mediated endocytosis in AP-2-depleted cells. J. Cell Biol. *162*, 909–918.

Nakatsu, F., *et al.* (2004). Defective function of GABA-containing synaptic vesicles in mice lacking the AP-3B clathrin adaptor. J. Cell Biol. *167*, 293–302.

Nazarian, R., Falcón-Pérez, J. M., and Dell'Angelica, E. C. (2003). Biogenesis of lysosome-related organelles complex 3 (BLOC-3): a complex containing the Hermansky-Pudlak syndrome (HPS) proteins HPS1 and HPS4. Proc. Natl. Acad. Sci. USA *100*, 8770–8775.

Nazarian, R., Starcevic, M., Spencer, M. J., and Dell'Angelica, E. C. (2006). Reinvestigation of the dysbindin subunit of BLOC-1 (biogenesis of lysosome-related organelles complex-1) as a dystrobrevin-binding protein. Biochem. J. *395*, 587–598.

Nie, Z., Boehm, M., Boja, E. S., Vass, W. C., Bonifacino, J. S., Fales, H. M., and Randazzo, P. A. (2003). Specific regulation of the adaptor protein complex AP-3 by the Arf GAP AGAP1. Dev. Cell *5*, 513–521.

Norton, N., Williams, H. J., and Owen, M. J. (2006). An update on the genetics of schizophrenia. Curr. Opin. Psychiatry *19*, 158–164.

Ooi, C. E., Dell'Angelica, E. C., and Bonifacino, J. S. (1998). ADP-ribosylation factor 1 (ARF1) regulates recruitment of the AP-3 adaptor complex to membranes. J. Cell Biol. *142*, 391–402.

Ozeki, H., Ito, S., Wakamatsu, K., and Hirobe, T. (1995). Chemical characterization of hair melanins in various coat-color mutants of mice. J. Invest. Dermatol. *105*, 361–366.

Peden, A. A., Rudge, R. E., Lui, W. W. Y., and Robinson, M. S. (2002). Assembly and function of AP-3 complexes in cells expressing mutant subunits. J. Cell Biol. *156*, 327–336.

Peden, A. A., Oorschot, V., Hesser, B. A., Austin, C. D., Scheller, R. H., and Klumperman, J. (2004). Localization of the AP-3 adaptor complex defines a novel endosomal exit site for lysosomal membrane proteins. J. Cell Biol. *164*, 1065–1076.

Perret, E., Lakkaraju, A., Deborde, S., Schreiner, R., and Rodriguez-Boulan, E. (2005). Evolving endosomes: how many varieties and why? Curr. Opin. Cell Biol. *17*, 423–434.

Raposo, G., Tenza, D., Murphy, D. M., Berson, J. F., and Marks, M. S. (2001). Distinct protein sorting and localization to premelanosomes, melanosomes, and lysosomes in pigmented melanocytic cells. J. Cell Biol. *152*, 809–823.

Raposo, G., Fevrier, B., Stoorvogel, W., and Marks, M. S. (2002). Lysosome-related organelles: a view from immunity and pigmentation. Cell Struct. Funct. *27*, 443–456.

Salazar, G., Craige, B., Love, R., Kalman, D., and Faundez, V. (2005a). Vglut1 and Znt3 co-targeting mechanisms regulate vesicular zinc stores in PC12 cells. J. Cell Sci. *118*, 1911–1921.

Salazar, G., Craige, B., Wainer, B. H., Guo, J., De Camilli, P., and Faundez, V. (2005b). Phosphatidylinositol-4-kinase type II α is a component of adaptor protein-3-derived vesicles. Mol. Biol. Cell *16*, 3692–3704.

Salazar, G., *et al.* (2006). BLOC-1 complex deficiency alters the targeting of adaptor protein complex-3 cargoes. Mol. Biol. Cell *17*, 4014–4026.

Starcevic, M., and Dell'Angelica, E. C. (2004). Identification of snapin and three novel proteins (BLOS1, BLOS2 and BLOS3/reduced pigmentation) as subunits of biogenesis of lysosome-related organelles protein complex-1 (BLOC-1). J. Biol. Chem. *279*, 28393–28401.

Stoorvogel, W., Oorschot, V., and Geuze, H. J. (1996). A novel class of clathrin-coated vesicles budding from endosomes. J. Cell Biol. *132*, 21–33.

Straub, R. E., Mayhew, M. B., Vakkalanka, R. K., Kolachana, B., Goldberg, T. E., Egan, M. F., and Weinberger, D. R. (2005). MUTED, a protein that binds to dysbindin (DTNBP1), is associated with schizophrenia. Am. J. Med. Genet. *138B*, 136 (abstract).

Talbot, K., *et al.* (2004). Dysbindin-1 is reduced in intrinsic, glutamatergic terminals of the hippocampal formation in schizophrenia. J. Clin. Invest. *113*, 1353–1363.

Theos, A. C., *et al.* (2005). Functions of adaptor protein (AP)-3 and AP-1 in tyrosinase sorting from endosomes to melanosomes. Mol. Biol. Cell *16*, 5356–5372.

Wei, M. L. (2006). Hermansky-Pudlak syndrome: a disease of protein trafficking and organelle function. Pigment Cell Res. *19*, 19–42.

Wu, X., Rao, K., Bowers, M. B., Copeland, N. G., Jenkins, N. A., and Hammer, J. A., III (2001). Rab27a enables myosin Va-dependent melanosome capture by recruiting the myosin to the organelle. J. Cell Sci. *114*, 1091–1100.